

Effect of thickness on the optical and electrical properties of aluminum zinc oxide nanostructured thin film deposited on polycarbonate substrate

AKBAR ESHAGHI*, HAJKARIMI MOHAMMAD

Faculty of Materials Science and Engineering, Malek Ashtar University of Technology, Shahin shahr, Esfahan, Iran

In this research, aluminum zinc oxide nanostructure thin films of various thickness (200, 250, 300 nm) were deposited on polycarbonate polymer substrates using a magnetron sputtering technique. The properties of the thin films were investigated by X-ray diffraction, Field Emission Scanning Electron Microscopy, X-ray Photoelectron Spectroscopy, UV-VIS-NIR spectrophotometer and four point probe method. X-ray diffraction pattern showed that the aluminum zinc oxide thin film included polycrystalline structure. The morphological results indicated that grain size increased as the thickness increased. The transmittance and sheet resistance of the aluminum zinc oxide thin films showed that aluminum zinc oxide thin films with 200 nm thickness had the highest transmission whereas aluminum zinc oxide thin film with 300 nm had the best conductivity.

(Received November 14, 2015; accepted February 10, 2017)

Keywords: Aluminum zinc oxide, Thin film, Optical properties, Electrical properties

1. Introduction

Transparent conducting films deposited on polymer substrates have many advantages in comparison to those deposited on glass substrate including light weight and small volume. They can be used in plastic liquid crystal display devices, transparent electrostatic discharge, and electromagnetic shielding materials, flexible photovoltaic devices, unbreakable heat reflecting mirrors [1-3]. For years, the most important material for a transparent conducting film is indium tin oxide (ITO), owing to its excellent electrical and optical properties. ITO is the most favorable TCO because of its excellent electro-optical properties, but it is limited to use due to high cost and future availability of indium and toxicity [4-5]. Because of these limitations, alternative TCO materials are being developed. Among these alternative materials, aluminum zinc oxide (AZO or Al doped zinc oxide) has attracted much attention as a transparent conductive material because of its low cost and wide availability of its constituent raw materials, as well as its comparable electro-optical performances to ITO. Besides, it is nontoxic and easy to fabricate [6-8].

Many techniques have been employed in the deposition of AZO films such as including magnetron sputtering, pulsed laser deposition (PLD), chemical vapor deposition (CVD), spray deposition and sol gel processes [9-12]. Among them, magnetron sputtering is considered to be a suitable technique owing to its inherent

characteristics such as high deposition rate, good controllability and scalability to large area [9]. It was found that the properties of AZO films are strongly dependent upon the preparation conditions such as the sputtering power, sputtering time, chamber pressure and substrate temperature. In addition, it is also found that thickness has an impressive effect on the electro-optical properties of thin films [9].

In this study, transparent conducting AZO thin films with different thicknesses were deposited on polymer substrates by magnetron sputtering. The influence of the thicknesses on the structure, morphology and electro-optical characteristics of the AZO thin film has been analyzed.

2. Experimental

Nanostructured AZO thin films of various thicknesses (200, 250, 300 nm) were prepared on polycarbonate (PC) substrates by using of a DC magnetron sputtering method (MSS160 model, High vacuum Technology Center, ACECR-Sharif University Branch, IRAN). The deposition rate and the thickness of the growing films were measured by the use of a quartz-crystal sensor, which was placed near the substrate. The AZO thin film preparation conditions in the sputtering method are indicated in Table 1.

Table 1. AZO thin film preparation condition

Target	Substrate	power W/cm ²	Sputtering gas	Base pressure	Work pressure
ZnO/Al ₂ O ₃ (98/2 wt.%)	PC	-	Ar	-	-

Before thin film deposition, the PC substrates were ultrasonically cleaned in a 1% neutral detergent solution and then plasma etched according to the specifications in

Table 2. The plasma treatment was used to improve the adhesion of the AZO thin film onto the PC substrates.

Table 2. Plasma etching procedure condition

power W/cm ²	Sputtering gas	Tem °C	Etching time(min)	Base pressure mbar	Work pressure
-	Ar/O ₂ (90/10)	40	10	1.5×10 ⁻⁵	2×10 ⁻²

The structure and morphology of the thin films were determined using a Bruker X-ray diffractometer (XRD, D8ADVANCE, Germany, Ni-filter, Cu K_α radiation $\lambda = 1.5406 \text{ \AA}$) and Field emission scanning electron microscopy (FE-SEM, Hitachi S4160, Cold Field Emission, voltage 20KV). The surface chemical composition of the AZO thin film was analyzed by the X-ray photoelectron spectroscopy (XPS) using an Al K_α source (1486.6 eV). The X-ray source was operated at 15 kV with a current of 10 mA. The XPS spectra were calibrated with respect to a carbon-1s peak at 285eV. The transmittance spectra and sheet resistance of the AZO thin films were obtained using UV-VIS-NIR spectrophotometer (Shimadzu UV-3100) and a four point probe method, respectively.

3. Results and discussion

The crystalline structure and preferred orientation of the AZO thin films were investigated by XRD. The XRD patterns of the AZO thin films deposited at different thicknesses, from 200 to 300 nm, are shown in Fig. 1. It can be seen that all films are polycrystalline and exhibit the ZnO hexagonal wurtzite structure. C-axis (002) diffraction peaks were observed in the all AZO thin films [9, 13]. In the spectra it also appeared that (103) peaks have relatively weak intensity [14].

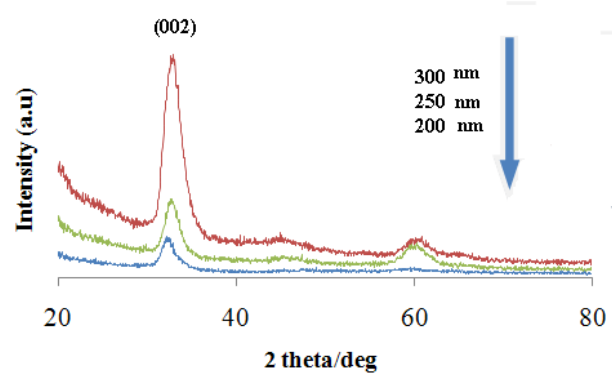


Fig. 1. XRD pattern of the AZO thin film

AZO thin films with high c-axis orientated crystalline structure along (002) plane can reduce the electrical resistivity due to an increase in carriers mobility by reducing the carriers scattering at the grain boundary [15]. The average crystallite sizes of the thin films were calculated from the Debye Scherer formula [16], using the (002) peak:

$$t = \frac{K\lambda}{\beta \cos \theta} \quad (1)$$

Where t is the crystallite size, K is a constant (0.9), λ is the wavelength of X-ray (Cu K_α-1.5406 Å), β is the half-peak width, and θ is the diffraction angle in degree.

The average crystallite sizes of the AZO thin films at different thicknesses are shown in Table 3. It can be seen that the average crystallite size increased by thickness increasing.

Table 3. Average Crystal size, grain size, and sheet resistance of the AZO thin films

Thickness(nm)	Crystal size (nm)	Grain size (nm)	Rs(Ω /Sq)	Transmittance (%) at 550 nm	FOM $10^{-4} \Omega^{-1}$
200	7.83	50	265	85	7.4
250	10.1	65	205	83	7.56
300	11.6	75	165	82	8.3

Fig. 2 shows FE-SEM images of the AZO thin films. It may be seen that the grain size of the AZO thin films increases along with an increase in the thickness. The average grain sizes of the AZO thin films are indicated in Table 3. This difference in the grain size is discussed in relation to the results of electro-optical characteristic of the AZO thin films in the following section.

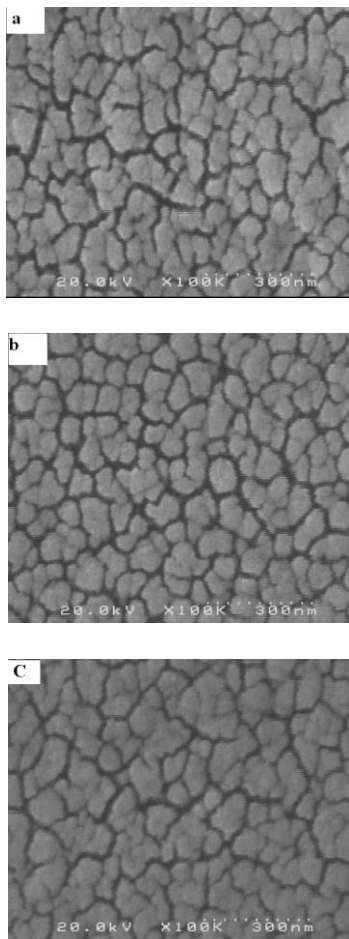


Fig. 2. FE-SEM images of the AZO thin films; a 200, b 250, c 300 nm

The XPS scan spectra of the AZO thin film (200 nm thickness) are shown in Fig. 3. Photoelectron peaks for Zn, O and C were recorded for the AZO film in the binding energy range of 0 to 1000 eV. The binding energy of the O 1s photoelectron peak is at 533 eV. A C 1s peak at a binding energy of 285 eV is observed on the film surface.

The binding energy of Zn 2p 3/2 at 1022.2 eV can be attributed to the Zn^{+2} bonding state from ZnO [14, 17].

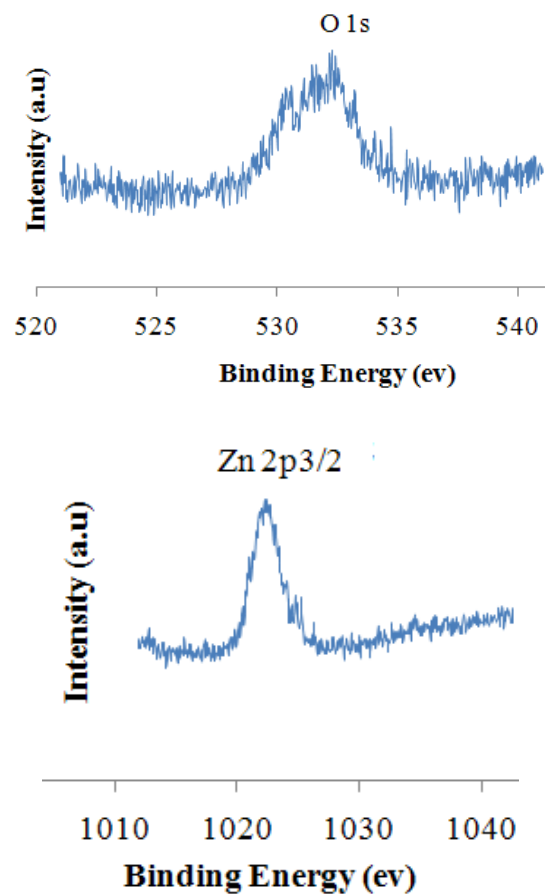


Fig. 3. XPS spectra of the AZO thin film, wide and narrow scan spectra

However, an attempt to detect aluminum and thereby predicting its chemical state in the prepared AZO films are not successful because of the low concentration of aluminum in the matrix.

AFM images are usually used to characterize the surface roughness. The surface roughnesses of thin films are indicated in Table 3. It can be seen from Table 3 that, as the thickness increases, grain size and then the RMS roughness increases [18].

Fig. 4 shows the transmittance spectra of the AZO thin films. It is clear that the transmittance of the AZO thin

film decreases when the thickness increases. This phenomenon can be related to the effect of grain size and surface roughness. When the thin film thickness increases, the grain size and surface roughness increases (see Table 3), which causes light scattering [3, 19].

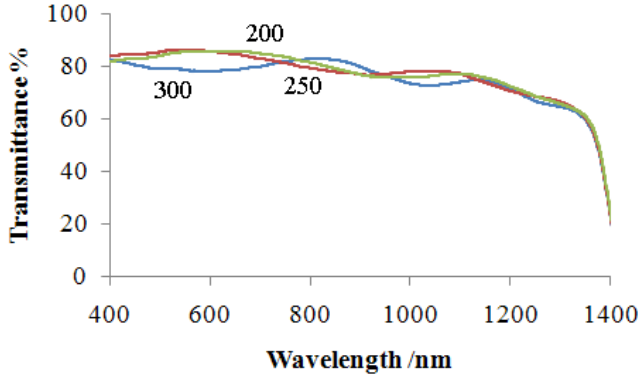


Fig. 4. Transmittance spectra of the AZO thin film

In addition, with increasing thickness, the average transmittance decreases slightly which may be caused by free carrier absorption that increases carrier concentration in thick film and leads to the absorption of more light [7]. In other words, the free carrier concentration increases with increasing thickness which contributes to the increasing absorption.

The sheet resistance (R_s) of the AZO thin films was measured by the four point probe method and the results are indicated in Table 3. The sheet resistance was found to be decreased with an increase in the thickness. It has been attributed to increase in the grain size which causes a weakening of the scattering among crystal grains. Similar type of result was noted by Shelke et al. [20].

According to Table 3, it is clear that there is an inverse relationship between the sheet resistance and grain size of the thin films. The sheet resistance of a thin film is expressed as:

$$R_s = 1/\sigma \quad (2)$$

where σ is the conductivity of the film. The conductivity is given by:

$$\sigma = nq\mu \quad (3)$$

where n is the free electron concentration, q is the electron charge and μ is the electron mobility. The electron mobility depends on several scattering mechanisms including lattice scattering, neutral impurity scattering and grain boundary scattering [19]. The grain boundary scattering is represented as [21]:

$$\mu_g = (\delta q) / (2\pi m_n^* kT) \exp(-\phi_b/kT) \quad (4)$$

Here δ is the grain size, m_n^* is the electron effective mass, ϕ_b is the grain boundary potential barrier, k is the Boltzmann constant and T is the absolute temperature. If the grain boundary scattering is considered to be the major

scattering mechanism, then the sheet resistance R_s can be indicated as:

$$R_s = 1/nq\mu_g t = 1/M\delta \quad (5)$$

Where $M = (nq^2 t) / (2\pi m_n^* kT)^{1/2} \exp(-\phi_b/kT)$

Thus, an inverse relationship between the sheet resistance and the grain size of the thin film can be anticipated. It is evident from Table 3 that the sheet resistances are more or less inversely related to the grain size. Therefore, the predominate mechanism of different conductivity is grain boundary scattering. Grain boundary can scatter the charge carriers. Thus, an increase in the film thickness leads to an increase of grain size and carrier motilities and hence to decrease of the electrical resistivity [21-22].

The quality of TCO films as transparent electrodes for electro-optical applications is evaluated generally by determining the relationship between the optical transmittance (T) and the sheet resistance (R_s) [23].

To evaluate the performance of transparent conducting films, Haake et al. [24] defined the figure of merit (FOM, Φ_{TC}), which is the ratio of the transmittance to sheet resistance. The figure of merit is given by the Haacke's formula:

$$\Phi_{TC} = \frac{T^{10}}{R_{sh}} \quad (6)$$

where R_{sh} is the sheet resistance and T is the optical transmittance at 550 nm.

The FOM values of the AZO thin films are given in the Table 3. The best FOM value for AZO thin film deposited on polycarbonate substrates is obtained at 300 nm thin film thickness. This indicates that high quality of AZO thin film deposited on polycarbonate substrate can be obtained in higher thickness.

4. Conclusion

In this research, AZO thin films with various thicknesses were deposited on polycarbonate substrates. The visible transmittance shows that transmittance decreases with film thickness. The sheet resistance measurement shows that thicker films have better electrical properties. It was confirmed that the electro-optical characteristics of the AZO thin films on polycarbonate substrates strongly depended on the film thickness.

References

- [1] A. Eshaghi, A. Graeli, *Optik* **125**, 1478 (2014).
- [2] A. Davoodi, M. Tajally, O. Mirzaee, A. Eshaghi, *Optik* **127**, 4645 (2016).
- [3] C. Guillen, J. Herrero, *Thin Solid Films* **480-481**, 129 (2005).
- [4] G. Fang, D. Li, B. L. Yao, *Vacuum* **68**, 363 (2003).
- [5] A. Eshaghi, M. J. Hakimi, A. Zali, *Optik* **26**, 5610 (2015).

- [6] A. Davoodi, M. Tajally, O. Mirzaee, A. Eshaghi, J. Alloy. Compound. **657**, 296 (2016).
- [7] F. Wang, M. Z. Wu, Y. Y. Wang, Y. M. Yu, X. M. Wu, L. J. Zhuge, Vacuum **89**, 127 (2013).
- [8] Y. S. Lin, S. Y. Lien, Y. C. Huang, C. C. Wang, C. Y. Liu, A. Nautiyal, D. S. Wu, S. J. Lee, Elsevier, Thin Solid Films **529**, 50 (2013).
- [9] S. Fernandez, A. Martinez-Steele, J. J. Gandia, F. B. Naranjo, Elsevier, Thin Solid Films **3152**, 517 (2009).
- [10] A. Illiberi, P. J. P. M. Simons, B. Kniknie, J. Deelen, M. Theelen, M. Zeman, M. Tijssen, W. Zijlmans, H. L. A. H. Steijvers, D. Habets, A. C. Janssen, E. H. A. Beckers, J. Crystal Growth **347**, 56 (2012).
- [11] P. Carreras, A. Antony, F. Rojas, J. Bertomeu, Elsevier, Thin Solid Films **520**(2), 1223 (2011).
- [12] D. Inamdar, C. Agashe, P. Kadam, S. Mahamuni, Elsevier, Thin Solid Films **520**(11), 3871 (2012).
- [13] A. I. Ali, J. Korean Phys. Soc. **49**, S652 (2006).
- [14] L. Gong, Z. Ye, J. Lu, L. Zhu, J. Huang, X. Gu, B. Zhao, Vacuum **84**, 947 (2010).
- [15] S. M. Hosseini Pilangorgi, F. Dehghan Nayeri, E. Asl-Soleimani, International Conference on Nanotechnology and Biosensors, 2011.
- [16] A. D. Achary, S. Moghe, R. Panda, S. B. Shrivastava, M. Gangrade, T. Shripathi, D. M. Phase, V. Ganesan, J. Mol. Struct. **1022**, 8 (2012).
- [17] S. H. Jeong, J. H. Boo, Elsevier, Thin Solid Films **447-448**, 105 (2004).
- [18] R. A. Mereu, A. Mesaros, M. Vasilescu, M. Popa, M. S. Gabor, L. Ciontea, T. Petrisor, Ceram. Int. **39**, 5535 (2013).
- [19] A. Eshaghi, M. Pakshir, R. Mozaffarinia, Elsevier, Appl. Surf. Sci. **256**(23), 7062 (2010).
- [20] V. Shelke, M. P. Bhole, D. S. Patil, Elsevier, Mater. Chem. Phys. **141**(1), 81 (2013).
- [21] A. K. Kulkarni, K. H. Schulz, T. S. Lim, M. Khan, Elsevier, Thin Solid Films **345**(2), 273 (1999).
- [22] M. Girtan, A. Vlad, R. Mallet, M. A. Bodea, J. D. Pedarnig, A. Stanculescu, D. Mardare, L. Leontie, S. Antohe, Elsevier, Appl. Surf. Sci. **274**, 306 (2013).
- [23] Z. Y. Zhong, T. Zhang, Mater. Lett. **96**, 237 (2013).
- [24] G. Haacke, J. Appl. Phys. **47**, 4086 (1976).

*Corresponding author: Eshaghi.akbar@gmail.com